Desalination and Water Treatment
www.deswater.com

doi: 10.1080/19443994.2013.766904

51 (2013) 7057–7066
November

Taylor & Francis
Taylor & Francis Group

Novel polyaniline/poly (vinyl alcohol)/clinoptilolite nanocomposite: dye removal, kinetic, and isotherm studies

A. Rashidzadeh, A. Olad*

Faculty of Chemistry, Polymer Composite Research Laboratory, Department of Applied Chemistry, University of Tabriz, Tabriz, Iran
Tel. +98 4113393164; Fax: +98 4113340191; email: a_oladgz@tabrizu.ac.ir

Received 4 November 2012; Accepted 10 January 2013

ABSTRACT

In this study, polyaniline/polyvinyl alcohol/clinoptilolite (PANI/PVA/Clino) nanocomposite was obtained by oxidative polymerization of anilinium cations inside and outside of the clinoptilolite channels. The structure and morphologies of the prepared nanocomposite were characterized by utilizing Fourier transform infrared spectroscopy and scanning electron microscopy. The prepared nanocomposite was used as an adsorbent for the removal of methylene blue (MB) dye from aqueous solutions. Furthermore, the adsorption kinetics studies showed that the adsorption process followed intraparticle diffusion model. Also, the investigation of adsorption isotherms showed that the equilibrium adsorption data were well described by the Langmuir isotherm model. It was concluded that chelating interaction between nanocomposite components and MB dye was the governing adsorption mechanism. Finally, desorption–adsorption cycle experiments showed that after 5 cycles; nanocomposite has a good adsorption behavior for MB dye and can be used as economic and efficient adsorbent.

Keywords: Nanocomposite; Polyaniline; Clinoptilolite; Methylene blue; Removal

1. Introduction

The increasing use of organic dye compounds in the paper, textile, food, and other industries causes pollution of the environment because of their non-biodegradability and high toxicity [1]. Several techniques are used for the removal of such hazardous contaminants from water. Among these methods, adsorption is probably the simplest process for the removal of dye compounds [2]. Among different adsorbents for the removal of environmental pollutants from water and wastewater, zeolites have drawn much attention in recent years [3]. Zeolites are microporous crystalline aluminosilicates that contain alkaline metal ions, water molecules, and three-dimensional network [4]. The three-dimensional framework of zeolites consists of nanometer-sized channels and cages, which endows high porosity and a large surface area in these materials, and makes them suitable for ion exchange and adsorption applications [5,6].

Because of low removal capacity of clinoptilolite, it was suggested to modify it with organic materials in order to increase pollutants uptake [7,8]. By exchanging the inorganic cations with organic cations, it is possible to convert a naturally hydrophilic property of

*Corresponding author.

zeolite into a hydrophobic and organophilic property [9]. In this regard, the zeolite has been ion exchanged with aniline hydrochloride in aqueous suspension and then oxidized to encapsulate polyaniline in the crystalline channel system of zeolite to form a hybrid nanocomposite [10,11]. The modified clinoptilolite zeolite with polyaniline was used for the removal of Cr (VI) from aqueous solutions by Olad et al. [12]. Polyaniline, because of its environmental stability, controllable quality, and good processability, have attracted great interest for the removal of pollutants from aqueous solution. To tackle the poor processability problems of polyaniline, synthesis of polyaniline in the presence of water soluble polymers like polyvinyl alcohol (PVA) or polyvinylpyrrolidone have been reported [13,14]. PVA is a nontoxic, water soluble, biocompatible and biodegradable synthetic polymer, which offers good tensile strength, flexibility, and barrier properties [15,16]. It was proven that the hydroxyl groups on PVA can also serve to adsorb heavy metal ions and anionic and cationic dyes [17,18]. PVA was crosslinked and blended with other polymers and was used for the adsorption of dye molecules [19,20]. It was reported that these composite adsorbents have good mechanical and chemical properties [21].

The aim of this study was to prepare an efficient adsorbent composed of polyaniline, PVA, and clinoptilolite. The prepared PANI/PVA/Clino nanocomposite was then applied for the removal of methylene blue (MB) dye as a model dye from aqueous solution. Effect of various parameters on removal efficiency as well as isothermal studies was investigated and reported.

2. Experimental

2.1. Reagents and materials

PVA, MB dye, ammonium persulfate, hydrochloric acid, and acetone were all purchased from Merck chemicals and were used as received. Aniline monomer from Merck was distilled prior to use. The natural clinoptilolite used in this study was obtained from Meianah mine in East Azerbaijan, Iran.

2.2. Instrumentation

A Fourier transform infrared (FT-IR) spectroscopy, Bruker Tensor 27 (Germany) was used to investigate the physicochemical interactions between organic and inorganic phases. An X-ray diffractometer (XRD) D500 Siemens (Germany) was used to study the crystallinity of materials. A scanning electron microscopy (SEM) LEO440i (England) was used to investigate the surface morphology of prepared nanocomposite coating. The UV–visible spectra of dye-containing aqueous solutions were recorded by use of a Shimadzu UV-1700 Pharma Spectrophotometer.

2.3. Synthesis of nanocomposite

To prepare acidic clinoptilolite, the natural zeolite rocks were first hammered to break down them into smaller particles. Then, the smaller particles were grinded and magnetically stirred for 48 h in HCl (0.1 M) solution. The slurry was then filtered and washed with excess deionized water until neutral, followed by drying at 150˚C for a period of 2 h. By acidifying the clinoptilolite zeolite, the adhesion of polymer to the zeolite can be increased.

In our approach, PANI/PVA/Clino nanocomposite was synthesized in the presence of PVA and clinoptilolite zeolite by insitu polymerization method. Clinoptilolite at weight ratios of 1, 3, and 5% (w/w) vs. aniline monomer was dispersed in 200 ml of HCl (1 M) solution containing aniline monomer and PVA (3%) solution. The mixture was magnetically stirred for 48 h at room temperature. Then, ammonium persulfate solution in 200 ml of deionized water was added drop wise for a period of 6 h to the mixture of anilinium cation and dispersion of clinoptilolite, while the reaction mixture vigorously stirred at −2 to −5˚C. The polymerization of anilinium cations in the clinoptilolite channels was carried out, and the nanocomposite of PANI/PVA/Clino was collected as precipitate. The precipitated nanocomposite was washed repeatedly with distilled water until the under washing solution became colorless followed by drying at 50˚C for 12 h.

2.5. MB adsorption and desorption experiments

The MB solutions were prepared in different concentrations ranged from 5 to 50 ppm by diluting of stock solution (1,000 ppm) appropriately using distilled water. Various amounts of nanocomposite powder were introduced with 50 ml of MB solutions of different concentrations. Then, the concentration of MB in solution was measured spectrophotometrically after different exposure times. The adsorption capacity was calculated by the following formula:

$$Q_e = \frac{(C_i - C_e)V}{m} \quad (1)$$

where Q_e = adsorption capacity or amount of dye adsorbed by adsorbent ($mg\,g^{-1}$), C_i = initial dye concentration (mgl^{-1}), C_e = equilibrium or residual dye concentration (mgl^{-1}), V = the volume of the solution (l), and m = mass of adsorbent (g). Also, the removal efficiency of MB was calculated according to Eq. (2).

$$\text{Removal efficiency} = \frac{C_i - C}{C_i} \times 100 \quad (2)$$

where C_i is the initial MB concentration, C is the concentration of unremoved MB after certain exposure time.

Desorption studies were performed by contacting used adsorbents with HCl (0.1 M) solution and agitated for 360 min. Then, the desorbed amount of MB was obtained spectrophotometrically. Desorption ration was calculated using Eq. (3):

$$\text{Desorption ratio} = \frac{C}{C_0} \times 100 \quad (3)$$

where C is the amount of MB dye desorbed to the elution medium, C_0 is the amount of MB dye adsorbed on the adsorbent.

To determine the reusability of the nanocomposite, consecutive adsorption–desorption cycle was repeated for five times with the same sample.

3. Results and discussion

3.1. FT-IR spectra

To get more insight into the bending and stretching vibrations, the PANI/PVA/Clino nanocomposite was characterized using FT-IR technique. Fig. 1 shows the FT-IR spectra of PVA, PANI, and PANI/PVA/Clino nanocomposite with 5% w/w clinoptilolite content. The FT-IR spectra of PVA shows major peaks related to hydroxyl and acetate groups. The sharp peak at 3,438 cm^{-1} is due to intermolecular H-bonded O–H stretching. The peaks at 2,940 and 2,913 cm^{-1} are assigned as alkyl C–H stretching vibration. The absorption peaks at 1,716 and 1,650 cm^{-1} correspond to C=O stretching and C–O stretching of acetate group [22]. An important absorption band related to carboxyl stretching band C–O is seen at a frequency of 1140 cm^{-1}, which is mostly attributed to the crystallization of PVA [23]. After the reaction, this absorption band was disappeared which was the evidence of interaction of PVA with other components through formation of hydrogen bonding by which the crystallization of PVA was decreased. In the case of PANI, the characteristic peaks corresponding to the quinoid ring and benzene ring were observed at 1,495 and 1582 cm^{-1}, respectively. The other peaks at 822, 1,308, 2,916, and 3,434 cm^{-1} can be assigned to the N–H out-of-plane bending, C–N stretching, aromatic C–H in-plane bending, C–H stretch, and N–H stretch, respectively [24]. FT-IR spectra of PANI/PVA/Clino nanocomposite exhibits bands characteristic of polyaniline and PVA as well as of clinoptilolite which confirms the presence of these components in the PANI/PVA/Clino nanocomposite. Also the peaks related to clinoptilolite, appeared at about 3,700 cm^{-1} are due to OH stretching vibration in (Al–OH–Al) and (Si–OH–Si), and the peak at 1,600 cm^{-1} is due to H–O–H bending mode. Finally, two distinct peaks were observed between 750 and 600 cm^{-1}, which are related to Si–O(Si) and Si–O(Al) stretching bridges, respectively [25].

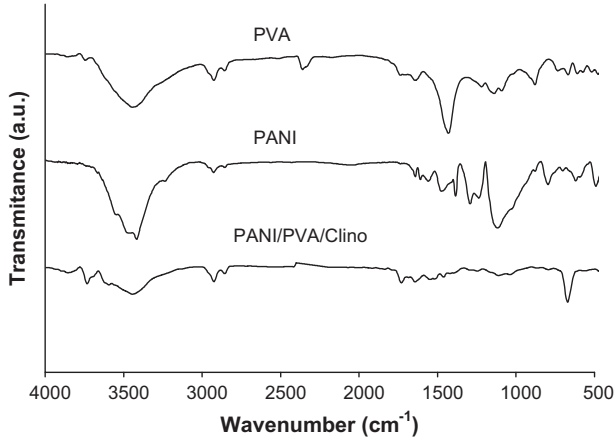

Fig. 1. FT-IR spectra of pure PVA, PANI, and PANI/PVA/Clino nanocomposite.

3.2. XRD patterns

Analysis of X-ray diffraction (XRD) patterns was used to investigate the structure and crystallinity of clinoptilolite and nanocomposite. The mineralogical

Table 1
Mineralogical composition of clinoptilolite

Composition	Percentage (%)	Composition	Percentage (%)
SiO_2	65	CaO	2.3
Al_2O_3	12.03	Fe_2O_3	1.5
K_2O	3	MnO	0.04
Na_2O	1.8	TiO_2	0.03
MgO	0.1	P_2O_5	0.01
L.O.I	12	–	–

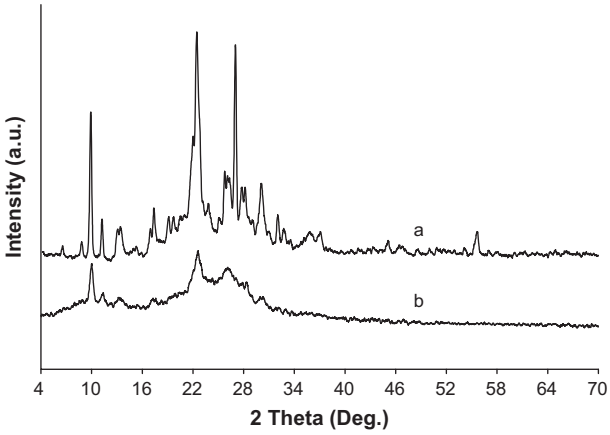

Fig. 2. XRD patterns of pristine clinoptilolite (a) and PANI/PVA/Clino nanocomposite (b).

composition of Meianah clinoptilolite has been shown in Table 1. Fig. 2 shows the XRD patterns of natural clinoptilolite (a) and PANI/PVA/Clino nanocomposite (b). The XRD pattern of clinoptilolite (Fig. 2(a)) shows the diffraction peaks appeared at $2\theta = 10.1^{\circ}$ and 22.67° due to the Miller indexes of 020 and 004, respectively [26]. Fig. 2(b) shows the XRD patterns of PANI/PVA/Clino nanocomposite. As it is known before, pure PANI because of its amorphous nature has a noncrystalline pattern, while the nanocomposite had the typical crystallite reflections associated with the zeolite component. The presence of the peaks related to the clinoptilolite in the XRD pattern recorded for PANI/PVA/Clino nanocomposite, confirms the presence of clinoptilolite in the nanocomposite composition.

3.3. Investigation of surface morphology

The surface morphology of polyaniline, clinoptilolite, and PANI/PVA/Clino nanocomposite was studied using SEM. The SEM image of clinoptilolite (Fig. 3 (a)) shows the layered structure of clinoptilolite with layer thicknesses in nanometer range. As can be seen in Fig. 3(b), SEM micrographs of polyaniline, reveal a globular morphology, with a particle diameter less than 100 nm. The SEM image of PANI/PVA/Clino nanocomposite (Fig. 3(c)) shows the presence of polyaniline on the layered surface of clinoptilolite. This image shows that the formation of polyaniline takes place not only in the clinoptilolite channels, but also on the clinoptilolite outside surfaces. This is due to the adsorption of anilinium cations both inside the channel surfaces and on the outside of clinoptilolite layers by the cation exchange processes between anilinium cations and the mineral cations existing in clinoptilolite channels.

3.4. Removal experiments

3.4.1. Adsorption kinetics

To evaluate the requisite time for nearly complete removal of MB and reaching adsorption equilibrium, 0.05 g of nanocomposite was exposed to a MB solution with the concentration of 10 ppm. The MB concentration was measured after different contact times. The removal efficiency was calculated using Eq. (1) and

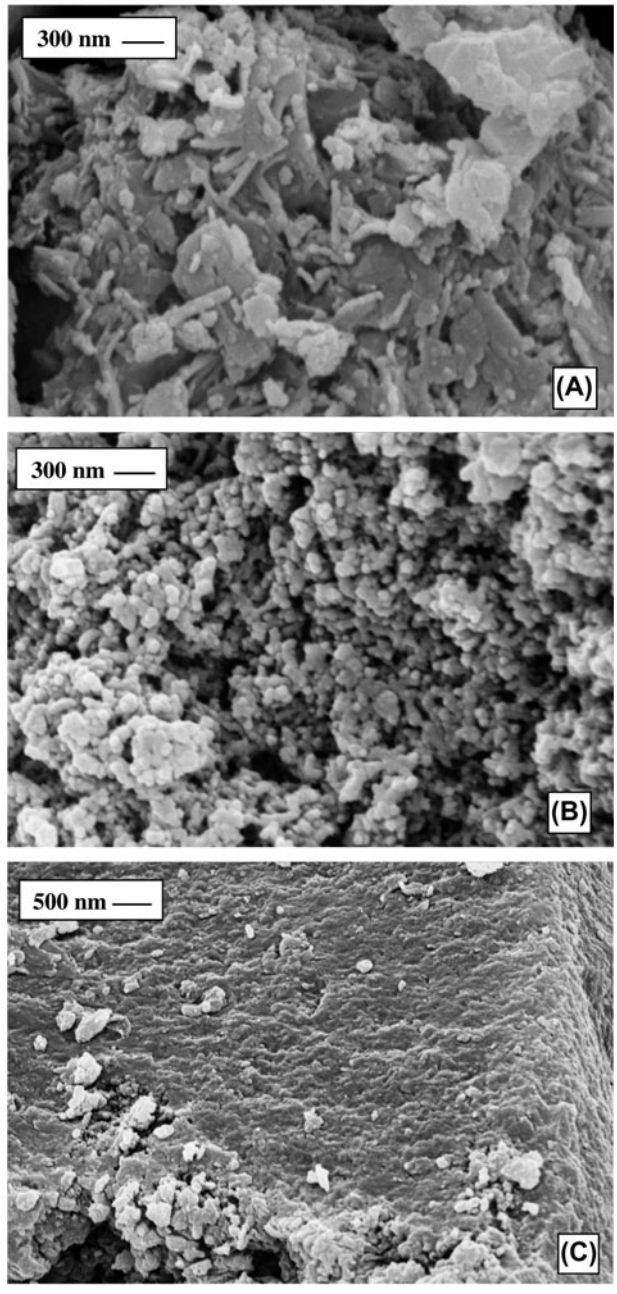

Fig. 3. SEM micrographs of (A) Clino, (B) PANI, and (C) PANI/PVA/Clino nanocomposite.

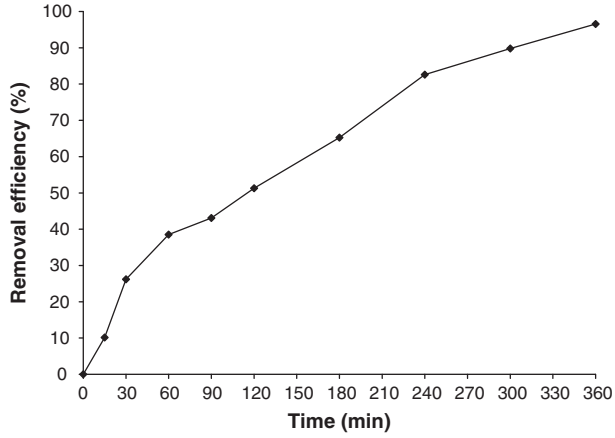

Fig. 4. The effect of contact time on the removal efficiency of MB.

plotted against time (Fig. 4). As shown in Fig. 4, after 360 min of exposure, over 95% of MB in the solution has been removed by nanocomposite powder. So, it can be concluded that 360 min is enough to remove over than 95% of MB from solution.

To investigate the adsorption mechanism, the kinetics of MB adsorption on nanocomposite was evaluated applying three different models: (1) the pseudo-first-order kinetic model [27], (2) pseudo-second-order kinetic model [28], and (3) intraparticle diffusion model [29,30] which were shown as below, respectively:

$$\log(q_e - q_t) = \log q_e - \frac{k_1}{2.303}t \quad (4)$$

$$\frac{t}{q_t} = \frac{1}{k_2 q_e^2} + \frac{1}{q_e}t \quad (5)$$

$$q_t = k_i t^{1/2} + C \quad (6)$$

where q_e is the adsorbed dye molecule concentration at equilibrium, k_1 is the rate constant of the pseudo-first-order sorption (min^{-1}), k_2 is the rate constant of the pseudo-second-order kinetics ($g\,mg^{-1}\,min^{-1}$), k_i ($mg\,g^{-1}\,min^{-1/2}$) is the intraparticle diffusion rate constant, and C ($mg\,g^{-1}$) is the constant which is related to the thickness of boundary layer.

The pseudo-first-order, pseudo-second-order, and intraparticle diffusion model have been applied to fit the experimental data (Fig. 5(a–c)), respectively, and their calculated parameters were all listed in Table 2. Based on the analysis of correlation coefficients (R^2), kinetic data of MB sorption on nanocomposite can be more appropriately defined by the intraparticle diffusion model since the correlation coefficient (R^2) value is higher than that of pseudo-first-order and pseudo-second-order models.

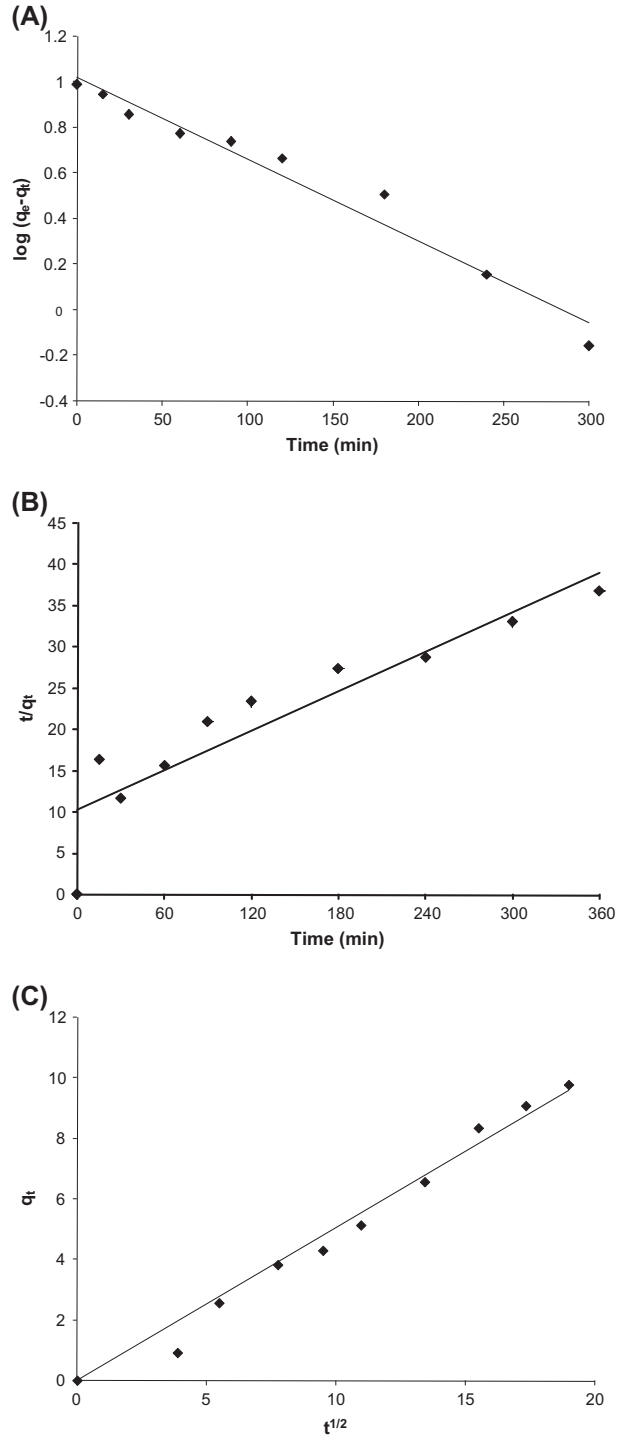

Fig. 5. Pseudo-first-order model (A), pseudo-second-order model (B), and intraparticle diffusion model (C).

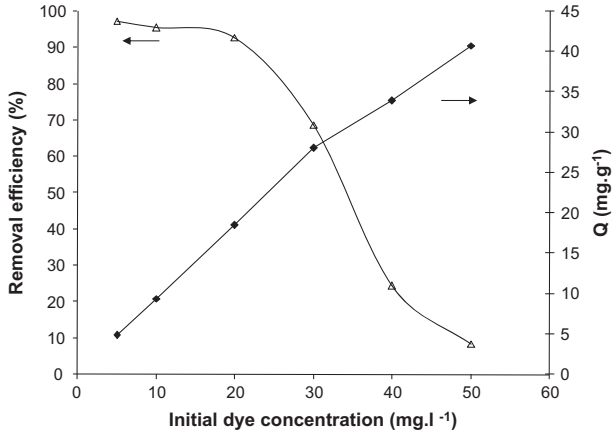

Fig. 6. The effect of initial concentration of MB on the removal efficiency of MB and adsorption capacity.

The intraparticle diffusion model provided the best correlation for all of the adsorption process and was predominant, whereas values of calculated q_e (10.502 mg g^{-1}) agreed with the experimental q (9.78 mg g^{-1}) in the case of pseudo-first-order kinetic. In addition, the intercept C proposed by Eq. (6) was zero for samples analyzed, and the line did pass through the origin, indicating that the intraparticle diffusion was the only rate limiting step and controlling factor in determining the kinetics of the adsorption process.

3.4.2. Effect of initial concentration of MB

To investigate the effect of initial concentration of MB on the removal efficiency of MB by hybrid nanocomposite, 0.05 g of nanocomposite powder was contacted for 360 min with 50 ml of MB solutions with different initial concentrations (5–50 ppm). As shown in Fig. 6, the removal efficiency decreased by increasing the initial concentration of dye solution which may be due to the saturation of adsorption sites on the nanocomposite adsorbent surface. At low concentration of dye, there will be unoccupied active sites on the adsorbent surface, and when the initial dye concentration increases, the active sites required for the adsorption of the MB dye molecules will decreases. However, with increasing initial concentration of dye, adsorption capacity increases. This may be due to the high driving force for mass at a high initial MB concentration. In other words, the residual concentration of MB molecules will be higher for higher initial MB concentrations. In the case of lower concentrations, the ratio of initial number of MB molecules to the available adsorption sites is low, and subsequently, the fractional adsorption becomes independent of initial concentration [31].

3.4.3. Adsorption isotherms

The adsorption isotherms of MB were simulated by the mathematical equations of Langmuir [32] and Freundlich [33]. The Langmuir model, which is presented in Eq. (7), suggests that the removal of dye occurs on a homogenous surface by monolayer sorption.

$$\frac{c_e}{q_e} = \left(\frac{1}{q_{max}}\right)c_e + 1/q_{max}b \tag{7}$$

where c_e (mgl^{-1}) is the equilibrium MB concentration, q_e (mg g^{-1}) is the amount adsorbed dye at equilibrium, q_{max} (mg g^{-1}) is the monolayer maximum adsorption capacity and b (1 mg^{-1}) is the Langmuir constant [34].

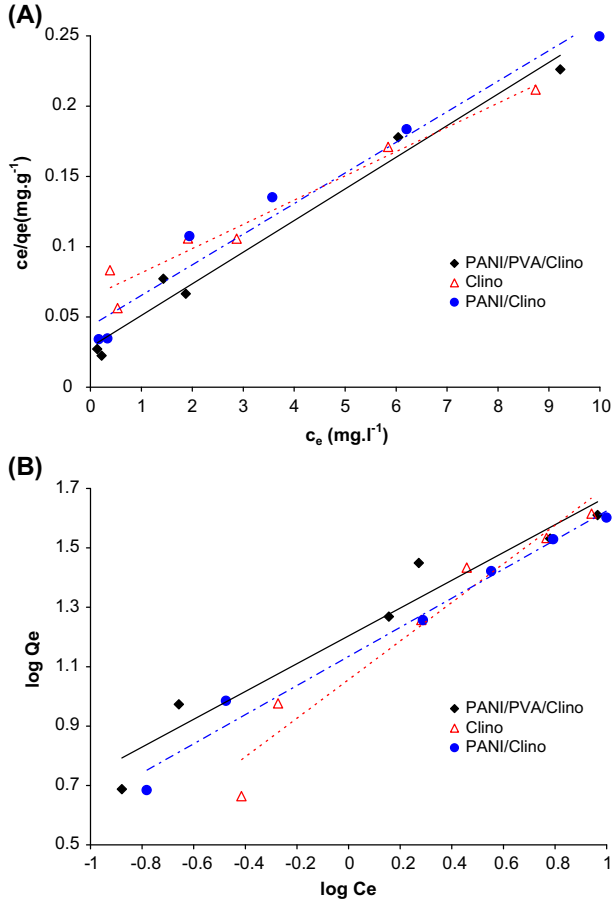

Fig. 7. Linearized forms of Langmuir (A) and Freundlich (B) isotherms for MB removal using different adsorbents.

Table 2
Parameters of pseudo-first-order, pseudo-second-order and intraparticle diffusion models for the adsorption of MB using PANI/PVA/Cino nanocomposite

Pseudo-first order			Pseudo-second order			Intraparticle diffusion		
R^2	Q_e(cal)	k_1	R^2	Q_e(cal)	k_2	R^2	C	K_i
0.9654	10.502	0.0083	0.842	12.531	0.000619	0.9804	0	0.505

The Freundlich model is used for the heterogeneous systems which active sites are distributed exponentially. This isotherm provides an empirical relationship between the sorption capacity and equilibrium constant of the sorbent [35]. The mathematical representation of this model is as follows:

$$\log q_e = \frac{1}{n}\log c_e + \log K_f \quad (8)$$

where K_f (mg g^{-1}) and n are the Freundlich constants related to adsorption capacity and adsorption intensity of adsorbents, respectively. The magnitude of n indicates that adsorption is favorable and values of $n > 1$ represent favorable adsorption condition. The obtained experimental data were fitted with the linearized forms of Langmuir and Freundlich models and were shown in Fig. 7(a) and (b) , respectively. To provide distinction between the different mechanisms and to indicate that which constituting materials dominates the adsorption process, information of MB adsorption to clinoptilolite alone, as well as MB adsorption to clinoptilolite with polyaniline was also presented. The corresponding correlation coefficients and the isotherm constants were calculated and presented in Table 3. As can be seen Table 3, in the case of PANI/PVA/Clino nanocomposite, the experimental data fit well with the linearized Langmuir isotherm, because the correlation coefficient for PANI/PVA/Clino nanocomposite (0.9804) is higher than that of Freundlich isotherm (0.9462). Also, calculated q_{max} from linearized Langmuir isotherm (44.44 mg g^{-1}) in the case of PANI/PVA/Clino nanocomposite is close to experimental amount of q (40.78 mg g^{-1}). However, in the case of PANI/Clino, maximum adsorption capacity is close to the value of q_{max} for PANI/PVA/Clino nanocomposite. Moreover, PANI/Clino shows slightly higher correlation coefficient (0.9651) in comparison with Clino (0.9623), which shows adsorption of dye on PANI has strong role on the overall adsorption of MB on PANI/PVA/Clino nanocomposite. On the other hand, in the case of Freundlich model, correlation coefficient of PANI/Clino is higher than that of Clino nanocomposite. This suggests that some heterogeneity in the surface or pores of PANI/Clino adsorbent as a result of addition of PANI will play a role in dye adsorption. Moreover, the Clino adsorbent presented lower K_f (11.378 mg g^{-1}) for MB than the PANI/PVA/Cino (15.98 mg g^{-1}) and PANI/Clino (13.62 mg g^{-1}). The K_f value can be correlated with the variation of surface area of the adsorbent [36]. Higher surface area of PANI/PVA/Cino nanocomposite will generally result in higher adsorption capacity [37]. The value of n, which is higher than 1, indicated that MB dye is favorably adsorbed by nanocomposite under the experimental conditions. However, the correlation coefficient obtained for PANI/PVA/Cino nanocomposite, PANI/Clino, and Clino using the Langmuir isotherm is higher than that for Freundlich isotherm suggesting higher probability of monolayer adsorption over multilayer adsorption [37].

3.4.4. Mechanism of adsorption

As it was seen, the prepared nanocomposite had high removal efficiency to remove MB dye from aqueous solutions. This can be related to the

Table 3
The parameters for Langmuir and Freundlich isotherms for MB removal using different adsorbents

	Langmuir isotherm			Freundlich isotherm		
	Q_{max}	b	R^2	n	K_f	R^2
PANI/PVA/Clino	44.44	0.78	0.9804	2.137	15.98	0.9462
PANI/Clino	45.87	0.43	0.9651	2.04	13.62	0.9798
Clino	57.80	0.27	0.9623	1.538	11.37	0.9484

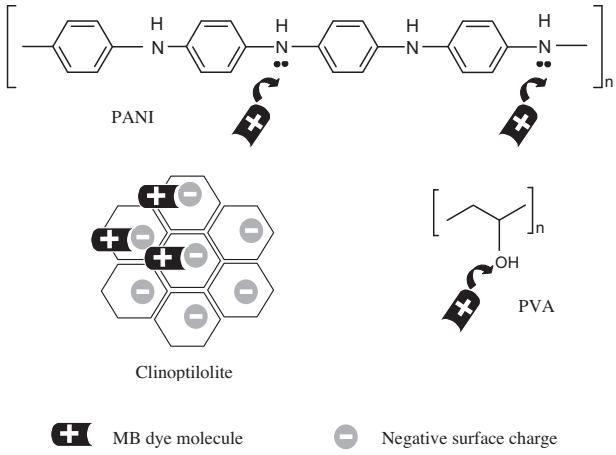

Fig. 8. Schematic illustration of adsorption of cationic MB dyes on to the prepared nanocomposite consisting of PANI, PVA, and Clino.

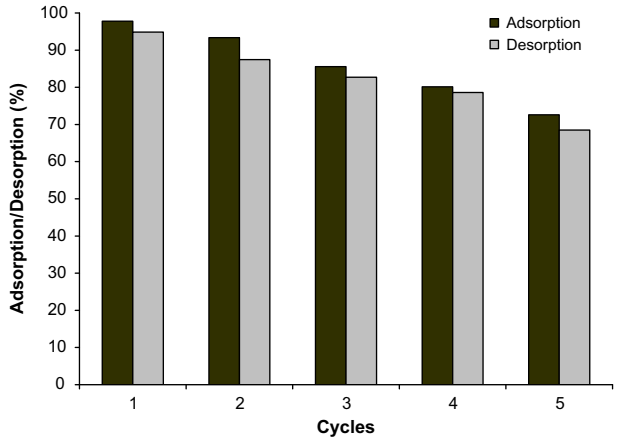

Fig. 9. Adsorption and desorption percent of MB dye in five cycles.

adsorbent which composed of different components which can be serving as adsorbent for dye individually. For example, polyaniline via its nitrogen atoms in amine derivatives forms coordinate bond with positive charge of MB dye ions. It is known that basic dyes or cationic dyes upon dissolution release colored dye cations into the solution. These dye cations can interact with the electrons in s^2p^3 orbital of nitrogen in polyaniline [38]. Also, the hydroxyl groups on PVA can also serve to adsorb cationic MB dye molecules. Natural zeolites like clinoptilolite have the negative surface charge. Consequently, positive charge dyes like MB adsorb on zeolite via electrostatic attraction. This process was schematically shown in Fig. 8. Therefore, it can be concluded that the type of interaction in this case can be described by chelation and ion exchange. As shown in previous section about adsorption isotherms, PANI/PVA/Cino nanocomposite has higher adsorption capacity in comparison with PANI/Clino and pristine Clino as adsorbent. High adsorption capacity indicates strong electrostatic force of attraction between dye molecules and sorbent binding sites as a result of addition of PANI and PVA [37].

Table 4
Adsorption capacities of different adsorbents for removal of MB

Adsorbents	Adsorption capacity ($mg\,g^{-1}$)	Sources
Clay	6.3	[39]
Poly (vinyl alcohol)	13.8	[31]
Kaolin	13.99	[40]
Natural tripoli	16.6	[41]
Polyethylene terephthalate	33.4	[42]
Polyaniline/sawdust	43.03	[43]
This work	44.44	–
Jordanian diatomite	88.6	[44]

3.4.5. Comparison of adsorption capacity with other similar systems

The maximum adsorption capacities of MB for the adsorbent used in this study along with other adsorbents were presented in Table 4. Although the adsorption capacity of PANI/PVA/Clino nanocomposite for MB was not that much high, it was much higher than that of other potential adsorbents such as clay [39], poly (vinyl alcohol) [31], kaolin [40], natural tripoli [41], polyethylene terephthalate [42], and polyaniline/sawdust [43]. According to the results obtained, PANI/PVA/Clino nanocomposite could be employed as an alternative adsorbent for the removal of MB.

3.4.6. Desorption and reusability studies

For practical applications, desorption experiments were performed to regenerate dye loaded nanocomposites. As mentioned previously, the PANI/PVA/Clino nanocomposite had high adsorption efficiency for MB dye and could adsorb about 98% of the MB dye. Therefore, the adsorption and desorption processes were repeated to examine the reusability potential of nanocomposite for economical purposes. Fig. 9 showed the adsorption and desorption percent of MB dye in five cycles. As shown in Fig. 9, the removal efficiency showed a little decrease in second cycle and reached 93% as a result of occupation of some

adsorption sites by MB dye. The removal efficiency and desorption ratio decreased per cycle, but in the fifth cycle, the adsorbent could remove about 73% of MB, meaning its high reusability. Loss of the adsorption capacity is due to the decrease in the availability of the number of adsorption sites for MB with increase in number of runs on the adsorbent. Furthermore, the results show that the adsorption in the next runs occurred only on the adsorption sites that were created due to the desorption of MB dye from the surface and pores of the PANI/PVA/Clino nanocomposite. Moreover, incomplete desorption could be attributed to the formation of very strong complexes between the functional groups of the adsorbents (like NH_2, OH) and MB.

4. Conclusion

The synthesis of PANI/PVA/Clino nanocomposite was performed by oxidative polymerization of anilinium cations inside and outside of the clinoptilolite channels in the presence of PVA. The application of prepared nanocomposite was investigated as an adsorbent for the removal of MB dye from aqueous solutions. It was found that the removal efficiency of MB using this nanocomposite powder as an adsorbent was about 98%. The batch sorption kinetics was tested and the pseudo-first-order kinetic model and intraparticle diffusion model were found to be the rate determining steps. The equilibrium data from experiments were analyzed by the Langmuir and Freundlich models that showed better fit with Langmuir model and monolayer adsorption. Desorption studies showed that after 5 cycles, nanocomposite had a good adsorption behavior for MB dye. Chelating interaction between nanocomposite components and MB dye was the governing adsorption mechanism.

Acknowledgment

The financial support of this research by the University of Tabriz is gratefully acknowledged.

References

[1] V.K. Gupta, Suhas, Application of low-cost adsorbents for dye removal—A review, J. Environ. Manage. 90 (2009) 2313–2342.
[2] S. Wang, Y. Peng, Natural zeolites as effective adsorbents in water and wastewater treatment, Chem. Eng. J. 156 (2010) 11–24.
[3] S. Wang, Z.H. Zhu, Characterisation and environmental application of an Australian natural zeolite for basic dye removal from aqueous solution, J. Hazard. Mater. B136 (2006) 946–952.
[4] M. Sprynskyy, M. Lebedynets, A.P. Terzyk, P. Kowalczyk, J. Namiesnik, B. Buszewski, Ammonium sorption from aqueous solutions by the natural zeolite transcarpathian clinoptilolite studied under dynamic conditions, J. Colloid Interface Sci. 284 (2005) 408–415.
[5] A.H. Oren, A. Kaya, Factors affecting adsorption characteristics of Zn^{2+} on two natural zeolites, J. Hazard. Mater. B131 (2006) 59–65.
[6] R. Patel, J.T. Park, H.P. Hong, J.H. Kim, B.R. Min, Use of block copolymer as compatibilizer in polyimide/zeolite composite membranes, Polym. Adv. Technol. 22 (2011) 768–772.
[7] B. Armagan, O. Ozdemir, M. Turan, M.S. Celik, The removal of reactive azo dyes by natural and modified zeolites, J. Chem. Technol. Biotechnol. 78 (2003) 725–732.
[8] M. Arora, N.K. Eddy, K.A. Mumford, Y. Baba, J.M. Perera, G. W. Stevens, Surface modification of natural zeolite by chitosan and its use for nitrate removal in cold regions, Cold Reg. Sci. Technol. 62 (2010) 92–97.
[9] M. Rozic, D. Ivanec Sipusic, L. Sekovanic, S. Miljanic, L.C. Urkovic, J. Hrenovic, Sorption phenomena of modification of clinoptilolite tuffs by surfactant cations, J. Colloid Interface Sci. 331 (2009) 295–301.
[10] A. Maity, N. Ballav, M. Biswas, Conducting composites of poly(N-vinylcarbazole), polypyrrole, and polyaniline with 13X-zeolite, J. Appl. Polym. Sci. 101 (2006) 913–921.
[11] T. Bein, P. Enzel, Encapsulation of polyaniline in zeolite y and mordenite, Synth. Met. 29 (1989) 163–168.
[12] A. Olad, M. Khatamian, B. Naseri, Removal of toxic hexavalent chromium by polyaniline modified clinoptilolite nanoparticles, J. Iran Chem. Soc. 8 (2011) S141–S151.
[13] J. Bhadra, D. Sarkar, Size variation of polyaniline nanoparticles dispersed in polyvinyl alcohol matrix, B. Mater. Sci. 33 (2010) 519–523.
[14] A. Olad, A. Rashidzadeh, Poly(N-vinylpyrrolidone) modified polyaniline/Na+-cloisite nanocomposite: Synthesis and characterization, Fiber Polym. 13 (2012) 16–20.
[15] R. Schellekens, C.J. Bastiansen, A drawing behaviour of polyvinyl alcohol fibers, J. Appl. Polym. Sci. 43 (1991) 2311–2315.
[16] H. Zheng, Y. Du, J. Yu, R. Huang, L. Zhang, Preparation and characterization of chitosan/poly(vinyl alcohol) blend fibers, J. Appl. Polym. Sci. 80 (2001) 2558–2565.
[17] S. Wu, F. Li, H. Wang, L. Fu, B. Zhang, G. Li, Effects of poly (vinyl alcohol) (PVA) content on preparation of novel thiol-functionalized mesoporous PVA/SiO_2 composite nanofiber membranes and their application for adsorption of heavy metal ions from aqueous solution, Polymer 51 (2010) 6203–6211.
[18] S.R. Sandeman, V.M. Gunko, O.M. Bakalinska, C.A. Howell, Y. Zheng, M.T. Kartel, G.J. Phillips, S.V. Mikhalovsky, Adsorption of anionic and cationic dyes by activated carbons, PVA hydrogels, and PVA/AC composite, J. Colloid. Interface Sci. 358 (2011) 582–592.
[19] M.M. Abd El-Latif, M.F. El-Kady, Amal M. Ibrahim, Mona.E. Ossman, Alginate/polyvinyl alcohol—Kaolin composite for removal of methylene blue from aqueous solution in a batch stirred tank reactor, J. Am. Sci. 6(5) (2010) 280–292.
[20] M. Zendehdel, A. Barati, H. Alikhani, A. Hekmat, Removal of methylene blue dye from wastewater by adsorption onto semi-inpenetrating polymer network hydrogels composed of acrylamide and acrylic acid copolymer and polyvinyl alcohol, Iran J. Environ. Health Sci. Eng. 7(5) (2010) 431–436.
[21] W.S. Wan Ngah, A. Kamari, Y.J. Koay, Equilibrium and kinetics studies of adsorption of copper (II) on chitosan and chitosan/PVA beads, Int. J. Biol. Macromol. 34 (2004) 155–161.
[22] S. Adhikari, P. Banerji, Polyaniline composite by *in situ* polymerization on a swollen PVA gel, Synth. Met. 159 (2009) 2519–2524.

[23] Y. Zheng, A. Wang, Removal of heavy metals using polyvinyl alcohol semi-IPN poly(acrylic acid)/tourmaline composite optimized with response surface methodology, Chem. Eng. J. 162 (2010) 186–193.
[24] P. Ghosh, S.K. Siddhanta, S.R. Haque, A. Chakrabarti, Stable polyaniline dispersions prepared in nonaqueous medium: Synthesis and characterization, Synth. Met. 123 (2001) 83–89.
[25] P. Castaldi, L. Santona, C. Cozza, V. Giuliano, C. Abbruzzese, V. Nastro, P. Melis, Thermal and spectroscopic studies of zeolites exchanged with metal cations, J. Mol. Struct. 734 (2005) 99–105.
[26] D. Baybas, U. Ulusoy, Polyacrylamide–clinoptilolite/Y-zeolite composites: Characterization and adsorptive features for terbium, J. Hazard. Mater. 187 (2011) 241–249.
[27] Y.S. Ho, C.C. Chiang, Sorption studies of acid dye by mixed sorbents, Adsorption 7 (2001) 139–147.
[28] Y.S. Ho, G. McKay, Pseudo-second order model for sorption processes, Process Biochem. 34 (1999) 451–465.
[29] W.J. Weber, J.C. Morris, Advances in water pollution research: Removal of biologically resistant pollutant from wastewater by adsorption, in: Proceedings of 1st International Conference on Water Pollution Symposium, vol. 2, Pergamon Press, Oxford, (1962) 231–266.
[30] W.J. Weber, J.C. Morris, Kinetics of adsorption on carbon from solutions, J. Sanit. Eng. Div. Am. Soc. Civ. Eng. 89 (1963) 31–60.
[31] S.A. Umoren, U.J. Etim, A.U. Israel, Adsorption of methylene blue from industrial effluent using poly (vinyl alcohol), J. Mater. Environ. Sci. 4(1) (2013) 75–86.
[32] N.A. Oztas, A. Karabakana, O. Topala, Removal of Fe(III) ion from aqueous solution by adsorption on raw and treated clinoptilolite samples, Micropor. Mesopor. Mat. 111 (2008) 200–205.
[33] E. Rosales, M. Pazos, M.A. Sanroman, T. Tavares, Application of zeolite-Arthrobacter viscosus system for the removal of heavy metal and dye: Chromium and Azure B, Desalination 284 (2012) 150–156.
[34] K.S. Hui, C.Y.H. Chao, S.C. Kot, Removal of mixed heavy metal ions in wastewater by zeolite 4A and residual products from recycled coal fly ash, J. Hazard. Mater. 127 (2005) 89–101.
[35] A. Krobba, D. Nibou, S. Amokrane, H. Mekatel, Adsorption of copper (II) onto molecular sieves NaY, Desalin. Water Treat. 37 (2012) 31–37.
[36] D.A. Fungaroa, L.C. Groschea, A.S. Pinheirob, J.C. Izidoroa, S.I. Borrely, Adsorption of methylene blue from aqueous solution on zeolitic material and the improvement as toxicity removal to living organisms. Orbital Elec. J. Chem., Campo Grande. 2 (3) (2010) 235–247.
[37] R. Ansari, Z. Mosayebzadeh, Application of polyaniline as an efficient and novel adsorbent for azo dyes removal from textile wastewaters, Chem. Pap. 65(1) (2011) 1–8.
[38] A.N. Chowdhury, S.R. Jesmeen, M.M. Hossain, Removal of dyes from water by conducting polymeric adsorbent, Polym. Adv. Technol. 15 (2004) 633–638.
[39] A. Gurses, S. Karaca, C. Dogar, R. Bayrak, M. Acıkyıldız, M. Yalcın, Determination of adsorptive properties of clay/water system: Methylene blue sorption, J. Colloid. Interface Sci. 269 (2004) 310–314.
[40] D. Ghosh, K.G. Bhattacharyya, Adsorption of methylene blue on kaolinite, Appl. Clay Sci. 20 (2002) 295–300.
[41] A.S. ALzaydien, Adsorption of methylene blue from aqueous solution onto a low-cost natural jordanian tripoli, Am. J. Environ. Sci. 5 (3) (2009) 197–208.
[42] F.S. Zhang, H. Itoh, Adsorbents made from waste ashes and post-consumer PET and their potential utilization in wastewater treatment, J. Hazard. Mater. 101 (2003) 323–337.
[43] M. Banimahd Keivani, K. Zare, H. Aghaie, R. Ansari, Removal of methylene blue dye by application of polyaniline nano composite from aqueous solutions, J. Phys. Theor. Chem. 6(1) (2009) 50–56.
[44] M.A. Al-Ghouti, M.A.M. Khraisheh, M.N.M. Ahmad, S. Allen, Adsorption behaviour of methylene blue onto Jordanian diatomite: A kinetic study, J. Hazard. Mater. 165 (2009) 589–598.